Dewetting: From Physics to the Biology of Intoxicated Cells

6

David Gonzalez-Rodriguez, Camille Morel, and Emmanuel Lemichez

Abstract

Pathogenic bacteria colonize or disseminate into cells and tissues by inducing large-scale remodeling of host membranes. The physical phenomena underpinning these massive membrane extension and deformation are poorly understood. Invasive strategies of pathogens have been recently enriched by the description of a spectacular mode of opening of large transendothelial cell macroaperture (TEM) tunnels correlated to the dissemination of EDIN-producing strains of *Staphylococcus aureus* via a hematogenous route or to the induction of gelatinous edema triggered by the edema toxin from *Bacillus anthracis*. Remarkably, these highly dynamic tunnels close rapidly after they reach a maximal size. Opening and closure of TEMs in cells lasts for hours without inducing endothelial cell death. Multidisciplinary studies have started to provide a broader perspective of both the molecular determinants controlling cytoskeleton organization at newly curved membranes generated by the opening of TEMs and the physical processes controlling the dynamics of these tunnels. Here we discuss the analogy between the opening of TEM tunnels and the physical principles of dewetting, stemming from a parallel between membrane tension and surface tension. This analogy provides a broad framework to investigate biophysical constraints in cell membrane dynamics and their diversion by certain invasive microbial agents.

D. Gonzalez-Rodriguez (✉)
Université de Lorraine, LCP-A2MC, Metz, France
e-mail: david.gr@univ-lorraine.fr

C. Morel
Unité des Toxines Bactériennes, Institut Pasteur, UMR CNRS 2001, Paris, France

Paris Diderot, Sorbonne Paris Cité, Paris, France

E. Lemichez (✉)
Unité des Toxines Bactériennes, Institut Pasteur, UMR CNRS 2001, Paris, France
e-mail: emmanuel.lemichez@pasteur.fr

Abbreviations

BAR	Bin Amphiphysin Rvs167 domain
EDIN	Epidermal cell Differentiation Inhibitor
HUVEC	Human umbilical vein endothelial cell
I-BAR	Inverse-BAR domain
MIM	Missing in metastatis

SNARE   Soluble NSF attachment protein re-
          ceptor
TEM   Transendothelial cell macroaperture

6.1   Introduction

Interfacial forces such as surface tension domi-
nate the physics at the micrometric scale, which is
characteristic of cellular objects. Indeed, surface
tension in liquids has led to two different biophys-
ical analogies in living systems. The first type of
analogy has been proposed for multicellular sys-
tems, such as multicellular aggregates (Steinberg
1963) or biofilms (Oldewurtel et al. 2015). In this
analogy, the cells or bacteria forming the mul-
ticellular system are identified to the molecules
of a liquid. Such units attract each other through
intercellular adhesion, similar to molecular inter-
actions in a liquid. A force imbalance arises at
the system's interface, where cells (molecules)
only have neighbors to one side. This imbalance
is energetically unfavorable and leads the units
to spontaneously reorganize to reduce the total
surface of the interface. This is the molecular
origin of surface tension that describes both the
behavior of a liquid drop and of a multicellu-
lar system. Thus, surface tension has been char-
acterized and measured for cellular aggregates
(Phillips and Steinberg 1978, Forgacs et al. 1988,
Guevorkian et al. 2010), soft tissues (Maitre et al.
2015), and bacterial colonies (Rühs et al. 2013).
The physical similarities between multicellular
systems and liquid drops have led to studying
the collective dynamics of multicellular systems
through analogies with wetting (Douezan and
Brochard-Wyart 2011, Gonzalez-Rodriguez et al.
2012a) and dewetting (Douezan and Brochard-
Wyart 2012). A second type of analogy has been
proposed at the scale of a single cell. The cell
is modeled as a viscous liquid drop (Yeung and
Evans 1989) and an analogy is established be-
tween liquid surface tension and membrane ten-
sion of cells. The idealized picture of a tense
membrane to conceptualize liquid surface tension
becomes here an actual tense membrane. Impor-
tantly, the effective membrane tension in the cell

is the sum of two different contributions, one
arising from the plasma membrane itself and the
other from the actin cortex, to which the plasma
membrane is attached (Sheetz and Dai 1996; Diz-
Muñoz et al. 2013). The analogy with surface ten-
sion is valuable to understand cell shape (Fischer-
Friedrich et al. 2014), cell adhesion (Sackmann
and Bruinsma 2002), or cell dewetting, which is
the topic of this chapter.

A liquid film forced to spread on a non-
wettable substrate may spontaneously withdraw
from the substrate, leading to the formation of dry
patches (Fig. 6.1). This phenomenon is known
as dewetting. The phenomenon of dewetting
is observed for example when placing a thin
layer of oil on a non-sticking pan. Dewetting is
driven by a difference in interfacial energies
of the liquid between wet and dry regions,
the wetting zone being favored. This energy
difference translates into tension driving the
motion of the liquid surface. The liquid surface
can be pictured as a tense membrane whose
tension will spontaneously tend to minimize the
liquid surface by forming dry patches. By analogy
with liquid dewetting, cellular dewetting refers
to the process of nucleation and enlargement
of transendothelial cell macroaperture (TEM)
tunnel observed in endothelial cells (Lemichez
et al. 2013) (Fig. 6.1). Several exoenzymes
and AB toxins from pathogenic bacteria have
the property to induce a cellular dewetting
of endothelial cells. They comprise EDIN-
like factors from *Staphylococcus aureus* and
Clostridium botulinum that inactivate RhoA as
well as cyclic-AMP producing adenylate cyclase
toxins from *Bacillus anthracis* and *Bordetella
pertussis*. Formation of TEM tunnels occurs
upon relaxation of the actomyosin cytoskeleton
as a result of (i) inhibition of the small GTPase
RhoA by mono-ADP-ribosylating toxins, (ii)
inhibition of the Rho kinase (ROCK) with the
Y27632 compound or (iii) a rise of intracellular
cyclic-AMP concentration (Boyer et al. 2006;
Maddugoda et al. 2011). Video microscopy
studies of the dynamics of TEM tunnel formation
have revealed the remarkable transient nature
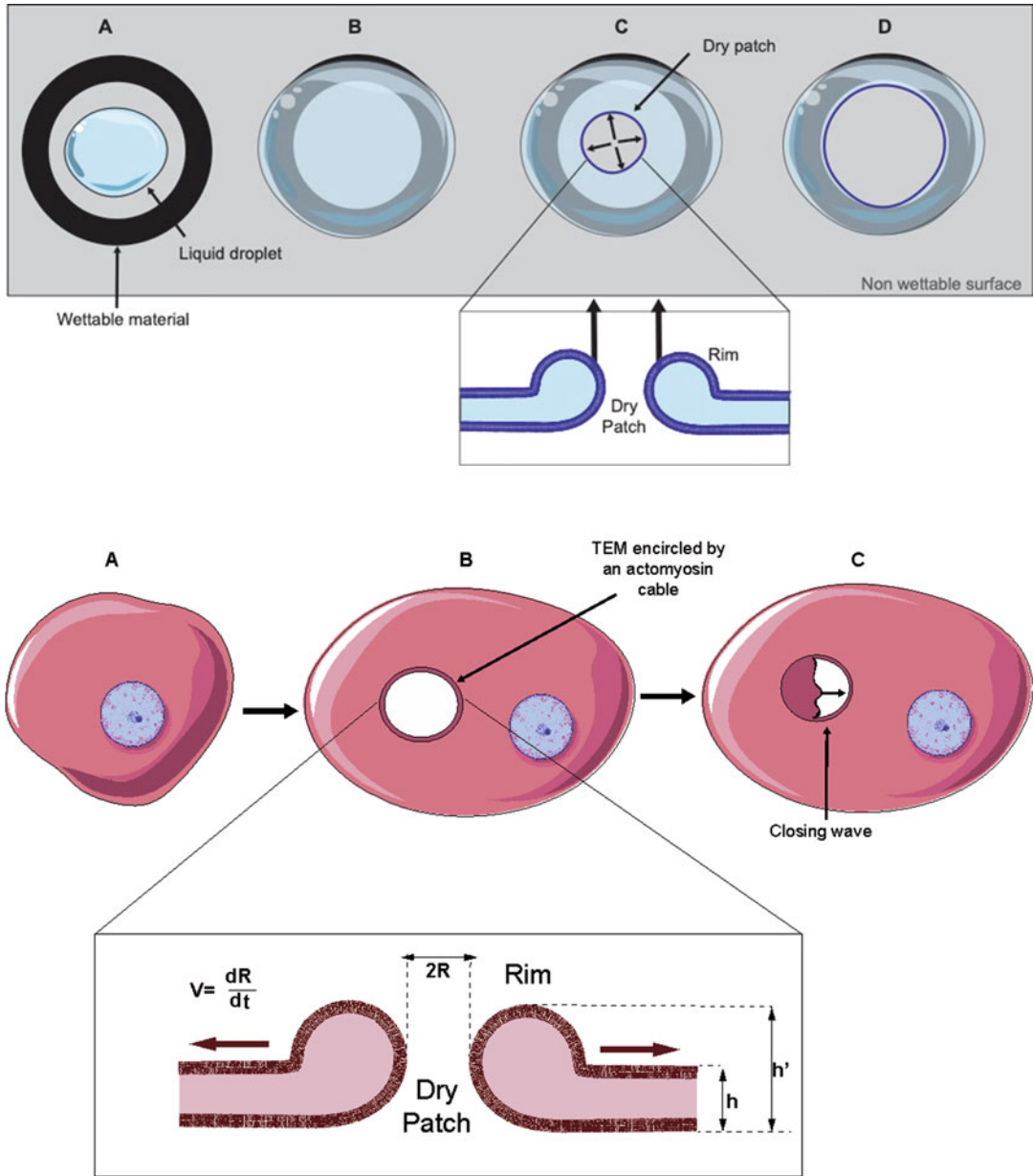of their opening (Fig. 6.2). Tunnels open and

Fig. 6.1 Physical process of liquid dewetting compared to biological cellular dewetting. Upper panel: dewetting phenomenon. (**a**) A liquid droplet is deposited at the center of a non-wettable surface, surrounded by a black region that has been rendered wettable. (**b**) The droplet is mechanically forced to spread and gets pinned by the wettable region, created by a localized substrate treatment. Thus, a metastable state is reached. (**c**) Nucleation of a dry patch destabilizes the system. The dry patch opens up spontaneously so that free energy is minimized. (**d**) The dry patch grows until it fully withdraws from the non-wettable zone. The liquid removed from the dry zone accumulates in a rim. Lower panel: cellular dewetting phenomenon. (**a**) An untreated cell with its nucleus (in blue). (**b**) Upon RhoA inhibiting exoenzyme treatment, the cell spreads thereby increasing membrane tension. A TEM forms and enlarges up to a maximal size, also displaying the formation of a rim along the TEM. The formation of a rigid actin cable encircling the TEM allows its stabilization. (**c**) TEMs open transiently owing to the formation of membrane waves invading the dry patch up to complete resealing of the TEM.(**d**) Schematic side-view showing characteristic dimensions (h = 50 nm, h' = 100 nm, t: time, R: radius, V: opening speed).
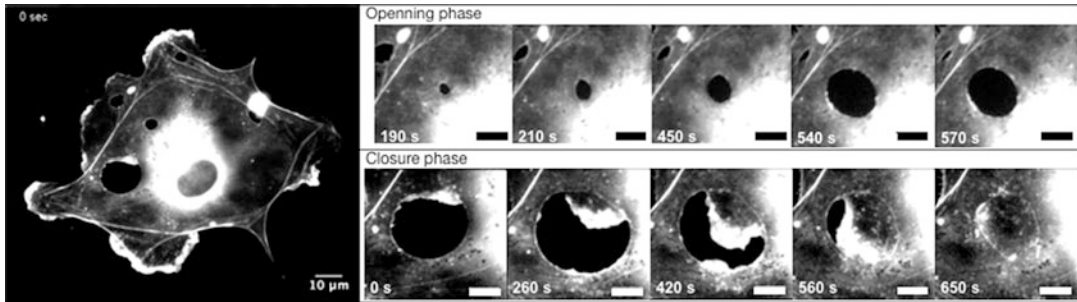
Fig. 6.2 Human Umbilical Vein Endothelial cell (HU-VEC) expressing pLifeAct-GFP intoxicated 24 h with edema toxin (ET) from *Bacillus anthracis* was imaged with a spinning-disk microscope (60×) at a rate of one image every 10 s during 1 h (Published in Maddugoda et al. 2011). Right panels show series of snapshots taken at the indicated time. It displays the opening (upper panel) and closure (lower panel) phase of two TEMs. The TEM opens and reaches its maximum size in a few tenths of seconds. Closure typically involves lamellipodia-like actin-rich membrane extension. Note the presence after closure of a persistent actin cable encircling TEMs. Scale bar represent 5 µm

enlarge in about 2 min before reaching a maximal radius of about 10 µm. After the tunnels have stabilized they undergo a phase of closure of about 3 min that involves the extension of membrane waves from their edges invading progressively the dry patch up to complete closure (Fig. 6.2) (Maddugoda et al. 2011). Cycles of TEM opening and closure occur for hours without induction of cell death or detectable leakage of cytosolic material (Boyer et al. 2006). *In vivo,* the expression of EDIN in a clinically relevant strain of *S. aureus* engineered to emit bioluminescence allows visualizing the resulting increase dissemination of bacteria through the vasculature tree forming more infectious foci in various tissues (Munro et al. 2010). Direct injection of EDIN or of the edema toxin from *B. anthracis* into the vasculature induces the loss of endothelium barrier integrity (Boyer et al. 2006; Maddugoda et al. 2011). *Ex vivo*, EDIN promotes the opening of large tunnels through the endothelium layer of vessels thereby unmasking the extracellular matrix fibers (Boyer et al. 2006). The formation of transcellular tunnels is not just a component of several infectious diseases. More broadly, transendothelial tunnels form during the diapedesis of leukocytes through the endothelium lining lymphatic and blood vessels (Alon and van Buul 2017). They also form in cells lining the Schlemm's canal, fulfilling an essential function in the transfer of aqueous humor from the eye chamber to the blood circulation (Braakman et al. 2014).

In this chapter, we review how the analogy with the physics of liquids has allowed a physical interpretation of the opening and enlargement phases of TEMs, yielding the name "cellular dewetting" (Gonzalez-Rodriguez et al. 2012b). While powerful, the analogy between liquid and cellular dewetting is not complete, as some physical aspects of cellular dewetting differ from liquid dewetting due to the intrinsic activity of living matter (Stefani et al. 2017). Here we review the physics of cellular dewetting in parallel to liquid dewetting. Through this parallel, we show the successes of the analogy and we also discuss physical aspects of liquid dewetting for which a cellular dewetting counterpart has not yet been described. This provides clues for future work to address several remaining open questions in the physics of living matter.

6.2 Physical Model of Cellular Dewetting

In this section we summarize the key ideas for the physical modeling of TEM opening arising from

an analogy with liquid dewetting. The driving force for cellular dewetting is

$$F_d = 2\sigma - \frac{T}{R}. \qquad (6.1)$$

Here σ is the membrane tension, which tends to open up a TEM and plays the role of the surface tension in liquid dewetting. Membrane tension is estimated to be of the order of 10^{-5} N/m (Raucher and Sheetz 2000). The factor of 2 in the equation reflects the existence of upper and lower membranes. T is the line tension that builds up at the edge of TEMs, when they enlarge. It arises from the energetic cost of forming the TEM edge, where the membrane is deformed to a very high curvature. While negligible in liquid dewetting, line tension plays an important role in cellular dewetting. R is the radius of the TEM. Eq. (6.1) may suggest that the line tension term becomes negligible for large TEMs. This is however not the case, because σ and T do not remain constant during the opening process, as discussed below. Spontaneous dewetting occurs when the driving force F_d is positive. This positive driving force arises from membrane tension increase due to the spreading of cells, but it can also be enhanced by externally applied equibiaxial strain, *i.e.* a strain of equal magnitude imposed along the two perpendicular directions on the sample plane (Braakman et al. 2014). Eq. (6.1) shows that $F_d > 0$ requires generating an initial TEM whose radius is larger than a certain threshold, $R > R_n = T/(2\sigma)$. This threshold for initiation of dewetting R_n is known as the nucleation radius. The calculated value of nucleation radius is of the order of 0.1 µm (Gonzalez-Rodriguez et al. 2012b), below photonic microscopy resolution, and its generation mechanisms remain incompletely described so far. As the TEM opens up, the membrane relaxes and membrane tension decreases. It can be assumed that this decrease of membrane tension is rather local given that meanwhile other TEMs open in the cells. Consistent with this notion, recent findings highlighted the local nature of membrane tension in cells (Shi et al.

2018). Moreover, line tension increases due to biological changes occurring around TEM perimeter, such as accumulation of scaffolding proteins (Gonzalez-Rodriguez et al. 2012b) and/or actin assembly (Stefani et al. 2017). As a result, the net driving force decreases and eventually becomes zero. Therefore, the TEM reaches a maximum size, at which spontaneous dewetting stops.

Physical models based on Eq. (6.1) have been developed to explain static aspects of the physics of TEM formation, the maximum size of TEMs, and the role of curvature-sensing proteins (Gonzalez-Rodriguez et al. 2012b, Stefani et al. 2017, Fedorov and Shemesh 2017). Similar to liquid dewetting, the dynamics of TEM opening are governed by a balance between the driving force in Eq. (6.1) and the dynamic resisting force arising from viscous dissipation (see Eq. 6.5 below). By using a viscous dissipation model, previous theoretical studies have described the experimentally observed dynamics of TEM opening (Gonzalez-Rodriguez et al. 2012a, b).

6.3 Characteristics of Cell Dewetting

After having discussed the general framework of the physical modeling of cellular dewetting, in this section we discuss in more detail the building blocks of the model, i.e. driving and resisting forces, nucleation, enlargement, reaching of a maximal size and closure of TEMs. We analyze the analogy between liquid dewetting and cellular dewetting and discuss the similarities and differences between the two. The reader interested in a more detailed overview of the physics of liquid dewetting is referred to the seminal book by P.-G. de Gennes and collaborators (de Gennes et al. 2003).

6.3.1 Driving Force

It has been hypothesized that the driving force for a cell to dewet is powered by an abnormal in-

crease of membrane tension, for example during cell stretching. In support of the role of membrane tension increase as a driver for TEM opening, *in vitro* observations highlight that mechanical stretching can induce tunnel formation. A monolayer of endothelial Schlemm's canal cells were cultured on a stretchable substrate and exposed to equibiaxial strain of up to 20%, which induced the formation of transcellular tunnels, as well as paracellular pores at cell junctions (Braakman et al. 2014). Similarly, the bacterial toxin EDIN induces a massive spreading of endothelial cells due to RhoA inhibition and downstream disruption of stress fibers. By analogy, the inhibition of NMII-dependent symmetric traction forces between opposite cell edges induces a sustained spreading of fibroblasts that likely tenses the membrane up to either a rupture of cell edges, which undergo retractions and adopt a C-shape, or the formation of intracelluar TEM-like gaps (Cai et al. 2010).

A major difference between TEMs that widen to reach a maximum size and holes in liquids that dewet completely arises from the characteristics of the driving force. The surface tension in liquid dewetting remains constant until the hole enlarges up to a complete disruption of the film. In contrast, membrane tension σ is related to the TEM radius R by Helfrich's law (Helfrich 1975):

$$\sigma = \sigma_0 \, \exp \left\{ -\frac{R^2}{R_c^2} \right\}, \qquad (6.2)$$

where σ_0 is the undisturbed value of the surface tension, in the absence of a TEM. The characteristic radius in the equation $R_c^2 = R_t^2 \left(k_B \hat{T} \right) / (8\pi\kappa)$, where R_t is the radius of the whole cell, $k_B \hat{T}$ is the thermal agitation energy, and κ is the membrane's bending rigidity. Equation (6.2) is obtained by considering all possible membrane fluctuation modes, whose energy scales as $k_B \hat{T}$ (equipartition theorem). The smallest possible fluctuation wavelength corresponds to the size of a membrane lipid molecule, whereas the largest possible fluctuation wavelength corresponds to the cell size, R_t. The thermal energy of the membrane fluctuations is used to stretch the membrane (work done

against the membrane tension σ) and to bend the membrane (work done against its bending rigidity κ). The mathematical formulation of these concepts leads to Eq. (6.2) (Helfrich 1975, Helfrich and Servuss 1984).

Helfrich's law is applicable to membranes subjected to thermal fluctuations. The law is also at play in pore formation in phospholipid vesicles (Sandre et al. 1999, Karatekin et al. 2003), which are are also transient. Opening of the hole is limited by reduction of surface tension as the pore opens and by line tension.

By injecting Eq. (6.2) into Eq. (6.1) and equating the driving force to zero, two equilibrium solutions for the TEM size are obtained. The smaller of them is the nucleation radius, R_n, and the largest of them is the maximum radius, R_m. For $R_n < R < R_m$, the driving force is positive and cellular dewetting proceeds spontaneously. The first physical model of cell dewetting showed that by combining the dewetting equation, Eq. (6.1), with Helfrich's law, Eq. (6.2), one can explain spontaneous TEM opening and the existence of a maximum TEM size (Gonzalez-Rodriguez et al. 2012b). This first result raised the question of the exact nature of line tension around TEMs.

TEM opening does not usually occur in isolation. Rather, it is observed that endothelial cells successively open TEMs at different locations. The opening of one TEM does not significantly impair further TEM opening in the cell. Interestingly, a recent study has provided evidence that membrane tension in cells is a local rather than a global parameter (Shi et al. 2018). According to this study, transmembrane proteins bound to the cytoskeleton act as an obstacle to the propagation of membrane tension variations. Thus, local perturbations in effective cell membrane tension require a time scale of the order of tenths of minutes to propagate to the whole cell, which is the same time scale required for TEMs to close back. This can explain why a local drop in membrane tension due to the opening of a TEM does not preclude subsequent TEM opening elsewhere in the cell.

Laser ablation experiments showed that TEMs having reached their maximum size resume opening when their periphery is perturbed (Stefani et al. 2017). Since laser ablation does

not modify membrane tension, these experiments demonstrated that membrane tension reduction does not suffice to explain TEM equilibrium size. This rather pointed to a key role of cytoskeletal-mediated line tension variations in the arrest of TEM enlargement.

6.3.2 Line Tension

Line tension is a force that acts around the edge of a dewetting hole to oppose its widening. In liquids, this force arises from the energetic cost needed to form a highly curved edge. The finding that TEMs stabilize has unveiled the importance of line tension to maintain the cellular integrity, i.e. prevent the extension of a TEM that would finally rupture the edge of cells. The origin of line tension in cell dewetting is a subject of ongoing research. To date, several mechanisms of line tension generation have been proposed: membrane-bending resistance, curvature-sensing proteins forming a scaffold stabilizing the periphery, and actomyosin cable assembly (Gonzalez-Rodriguez et al. 2012b, Stefani et al. 2017).

Membrane bending resistance is responsible for line tension in stretched vesicles (Sandre et al. 1999). When a pore is opened on a vesicle, the lipid molecules along the edge of the pore must curve with a very small radius of curvature that scales as the membrane thickness. This line tension induces the closure of transient pores in vesicles, where it is increased by inclusion of cholesterol and decreased by the addition of detergents (Karatekin et al. 2003). In the case of TEMs, the contribution of membrane bending to line tension is (Gonzalez-Rodriguez et al. 2012b):

$$T_{mb} = \frac{2\kappa}{h}. \qquad (6.3)$$

As captured by Eq. (6.3), the relevant radius of curvature of the membrane at the TEM border scales as the cell thickness h. Toxins that induce TEM formation perturb the cell cytoskele-ton, leading to a very flat morphology, with a typical thickness $h \sim 50$ nm. Thus, with an estimate of the membrane bending rigidity of $\kappa \sim 40\, k_B \hat{T}$, the membrane bending contribution to line tension is of the order of $T_{mb} \sim 5$ pN. This value is probably greater if one takes into account the force required to deform the cortical cytoskeleton. It is noted that line tension induced by membrane bending rigidity is smaller in TEM opening than it is in pores, because in TEMs the relevant radius for membrane bending is the endothelial cell thickness, whereas at pore edges the lipid membrane bends over itself to join the inner and outer leaflets. Line tension in TEMs arises from the bending rigidity of the whole membrane, similar to the line tension described at the edges of adherent cells (Oakes et al. 2014). This difference with pore opening leads to a significantly different value of h in Equation (6.3), and thus to a smaller line tension for TEMs (note that the relevant membrane bending rigidity is also different). However, line tension generation in TEM opening can also be mediated by other mechanisms that are absent in pore formation, as we discuss next.

Curvature-sensing by proteins such as Inverse-BAR domain (I-BAR)-containing proteins may enhance line tension (Saarikangas et al. 2009; Gonzalez-Rodriguez et al. 2012b). Association of these proteins to the TEM edge may increase the energetic cost of forming a border. Indeed, these proteins have a preferred spontaneous curvature that may deviate from the actual radius. An increase of the radius may thus force them to an unfavorable configuration, which would translate into a line tension. Interestingly, high-rate video acquisition showed that the I-BAR domain of MIM starts to accumulate along TEM edges a few hundred milliseconds after opening (Maddugoda et al. 2011). The size of TEMs increases upon depletion of the curvature-sensing protein MIM, which can be explained by a decrease of line tension (Maddugoda et al. 2011, Gonzalez-Rodriguez et al. 2012b).

Line tension is primarily provided by local actin reorganization around the TEM edges. It has been shown that an actomyosin cable encircles the TEMs as they open (Stefani et al.

2017). Laser ablation nano-surgery has revealed that cutting the actomyosin cable resumes TEM enlargement up to actomyosin cable formation at the edge of the enlarged zone. Line tension arising from the actomyosin cable limits TEM opening by opposing membrane tension, leading to TEM stabilization at a maximum size. Consistently, the introduction of a break in the cable by a laser nanosurgery-based approach promotes further widening of the hole until a new equilibrium state is reached (Stefani et al. 2017). Indeed, a new breaking then induces a second phase of TEM enlargement. The role of this cable in limiting TEM size in cellular dewetting can be expressed as an actomyosin contribution to the line tension, T_{am}. The actin scaffold is not present when the TEM nucleates, but rather it is recruited over time, leading to a time-dependent contribution to line tension, $T_{am} = T_{am}(t)$.

Stefani and collaborators have investigated the quantitative dependence of line tension on actomyosin cable formation, by combining physical modeling with experiments of TEM opening after laser ablation of the cable (Stefani et al. 2017). The predictions of different empirical models of line tension evolution were compared to experimental measurements of TEM opening after ablation. One such model assumed that T_{am} arises from the bending resistance of the cable. Another model supposed that the cable strengthens due to filamentous actin recruitment by convective sweeping of the cell cortex by the moving cable. These two models yielded predictions in contradiction with experimental data showing that the size increase of the TEM after ablation does not depend on its initial size, but it is rather a constant increment. In contrast, good experimental agreement was achieved by a third model that supposed a constant rate of increase of line tension over time, $T_{am} = \alpha t$, corresponding to a constant strengthening of the cable due to actin polymerization and bundling. These descriptions remain empirical, and a full quantitative understanding of the mechanisms by which actomyosin cable assembly leads to line tension generation is still lacking.

6.3.3 Nucleation

The mechanism of nucleation of these structures is probably the most fascinating and difficult question to address. Physical models can guide the response. According to Eq. (6.1), a TEM will open up if its size is larger than a certain threshold, known as the minimal nucleation radius R_n, which is estimated to be of the order of 0.1 µm (Gonzalez-Rodriguez et al. 2012b). The mechanism of TEM nucleation, i.e., of formation of the initial tunnel, remains incompletely understood. Even at the cellular scale, a systematic statistical investigation of a population of TEM nucleation events and a comparison with nucleation in classical liquid dewetting is still lacking. At the subcellular scale, TEM nucleation is probably enabled by thermal fluctuations of the two membranes. Because TEMs form in regions where the cells are very thin, the distance between the upper and lower cell membranes (~50 to 100 nm) is comparable to the amplitude of membrane fluctuations (Chen et al. 2009), which would allow the two membranes to meet. As the two inner leaflets meet, their fusion may be mediated by fusogenic proteins such as SNAREs (Carman and Springer 2008, Carman 2009) or by cations (Mondal Roy and Sankar 2011). In normal endothelial cells, cytoskeletal resistance to deformation is probably the main barrier to membrane fusion. Indeed, TEMs occur in intoxicated cells whose cytoskeleton is significantly perturbed, leading to a drop of the cell's elastic modulus, as measured by atomic force microscopy (Ng et al. 2017). Moreover, Ng and collaborators measured a lower penetration work to form TEMs in EDIN-treated cells. In contrast, direct ROCK inhibition has no impact on the penetration force required to form TEMs. This points toward the importance of other RhoA effectors than ROCK for example implicated in actin filaments polymerization and forming a viscous physical barrier to membrane fusion. The contributing role of the dynamics of cortical cytoskeleton in the initiation of tunnels is less defined. More broadly, one can

speculate that the formation of a dense network of branched actin filaments triggered by Arp2/3 at the interface of membranes also serves as a natural barrier to prevent membrane interaction and opening of TEMs.

Transcellular tunnel opening can also be induced by leukocytes during transmigration, a process in which leukocytes exert forces on endothelial cells through protrusions known as podosomes (Carman et al. 2007, Carman and Springer 2008). By analogy, it has been shown that the application of a mechanical force at the apical side of cells can overcome cytoskeletal resistance to membrane fusion and induce tunnel formation (Ng et al. 2017). In the experiments by Ng et al., compressive forces applied by means of an AFM tip on endothelial cells induced TEM nucleation. Interestingly, control endothelial cells respond to compression by actin polymerization that opposes TEM nucleation, whereas actin polymerization is impaired in intoxicated cells and TEMs open. These tunnels close like those induced by the toxin but are much less wide. The size of the AFM tip is comparable to the size of leukocyte podosomes, and the compression force required to induce TEM opening in AFM experiments (5–100 pN) is also comparable to the forces applied by podosomes during leukocyte transcellular diapedesis (Labernadie et al. 2014).

6.3.4   Maximum Size

Typical TEMs open up to a maximum size of the order of several micrometers. TEMs remain at their maximum size for a few tenths of seconds or minutes, before starting to close down. Closure is a slower process, typically lasting for a few minutes, and it is associated to the formation of lamellipodia-like actin-rich membrane waves for a majority of TEMs, whereas other close by a purse-string mechanism (Fig. 6.2).

The existence of a maximum size is a specific feature of cellular dewetting. The tunnels remain stably open when the cell is depleted of the MIM protein, showing that cell activity is required for the closure. In contrast, liquid dewetting is irre-versible, as dry patches continue to grow until the liquid has completely withdrawn from the non-wettable surface. In lipid vesicles, pore opening is also transient, but unlike TEMs no durable sta-bilization at a maximum size is observed between the opening and closure stages (Sandre et al. 1999). Stabilization of a dewetting hole is how-ever observed in liquid dewetting over a rough surface (de Gennes et al. 2003), although such stabilization arises from surface heterogeneities and not from the system itself, as in the process of cellular dewetting.

The maximum size of TEMs results from bal-ance between membrane tension and the kinetics of line tension increase. It corresponds to $F_d = 0$ in Eq. (6.1). In a configuration where membrane tension variations dominate over line tension, the maximum radius would scale as

$$R_m \sim R_c \left(- \ln \frac{T}{2\sigma_0 R_c} \right)^{1/2}. \qquad (6.4)$$

As discussed in the section on line tension above, the assumption of a constant line tension, arising from membrane bending resistance, satisfactorily predicts the typical size attained by TEMs formed *ex novo* (Gonzalez-Rodriguez et al. 2012b). However, this simple picture does not suffice to explain experimental observations of *de novo* TEM opening following laser ablation (Stefani et al. 2017), which requires accounting for a time-varying line tension provided by the assembly of an actin cable around the TEM. With this improvement, the cellular dewetting model can explain quantitatively the increase of TEM size following laser ablation (Stefani et al. 2017). It also provides a physical framework to our hypothesis that ezrin, a member of the FERM-domain containing protein family encompassing ezrin, radixin and moesin, specifically drives the formation of the actin cable encircling TEMs. Ezrin has a tendency to accumulate around TEMs, especially when phosphorylated on T567 (Tsai et al. 2018; Stefani et al. 2017). Ablation of ezrin leads to a higher turnover of F-actin around TEMs and the formation of TEMs of wider size. Taking into account a kinetic parameter in the line tension increase offers a theoretical framework

to the observation that a TEM opening *de novo* stabilizes to a maximal size while laser ablation-mediated disruption of the actin cable induced a widening of TEMs that is no longer limited. This particular case indicates that a major difference between viscous liquid dewetting and cellular dewetting comes from cytoskeletal-mediated line tension buildup at curved membranes, which stabilizes newly formed cell borders generated by the opening of TEMs.

6.3.5 Rim Formation

In classical liquid dewetting, the liquid removed from the dry patch accumulates in a rim that forms along the border of the hole (Redon et al. 1991, de Gennes et al. 2003). Such a liquid rim typically has a circular cross-section, and it increases in both height and width as dewetting proceeds, due to mass conservation.

Rim formation is also observed in cellular dewetting, as it has been evidenced by AFM profiles (Maddugoda et al. 2011). The rim appears to correspond to the accumulation of cytoplasmic material that has been displaced as the TEMs open (Gonzalez-Rodriguez et al. 2012b), see Fig. 6.1. Typical rim dimensions are about 100 nm in height and about 1 micrometer in width, whereas the cell height at the location of the tunnels is about 50 nm (measured with AFM operated at constant force of 100 pN, 0.3–1 Hz) (Maddugoda et al. 2011). A numerical model that accounts for membrane bending rigidity, membrane tension and cytoplasmic pressure explained the shape of the rim profile by free energy minimization (Fedorov and Shemesh 2017).

6.3.6 Viscous Dissipation and Opening Dynamics

During TEM opening, the driving force in Eq. (6.1) is positive. At the small length scales of TEM opening, this positive driving force cannot be balanced by inertia as in the macroscopic world. Indeed, the relevant Reynolds number for TEM opening is very small, of the order of 10^{-6}, indicating that inertial effects are negligible.

Therefore, the positive driving force must be balanced out by viscous dissipation, same as in viscous liquid dewetting.

In the study of viscous liquid dewetting, different scenarios have been described (de Gennes et al. 2003). For very thin films, where gravity effects are negligible, placed on a smooth and homogeneous solid substrate, liquid removed from the dry patch accumulates in a rim of circular cross-section. Viscous dissipation is mainly due to fluid flow within the rim. This scenario leads to a constant velocity of dewetting, $v = dR / dt = $ constant (Redon et al. 1991).

A second liquid dewetting scenario arises at longer time scales, once enough liquid has accumulated in the rim and gravity effects are no longer negligible. In this regime, the rim's cross-section becomes a flat pancake, with a maximum thickness equal to e_c, the critical thickness below which a liquid film dewets. This critical thickness scales as the capillary length, of the order of a millimeter. In this regime, viscous dissipation is concentrated at the wedges of the flat pancake, which leads to a law of dewetting of the form $R^2 = D.t$, where D is a constant (Brochard-Wyart et al. 1988).

A third scenario, which inspired the original analogy with cellular dewetting, is the dewetting on a slippery substrate, such as ultra-viscous liquid PDMS on a smooth and passive surface. It has been shown that ultra-viscous liquids slide over smooth, passive surfaces (Redon et al. 1994). Unlike the usual velocity profile of a viscous flow, where velocity vanishes at contact with the substrate due to the no-slip boundary condition, ultra-viscous liquids adopt a plug flow, with a constant velocity profile over the height. In this case, friction dissipation is given by

$$F_v \sim k\, l\, v, \tag{6.5}$$

where l is the width of the rim, $v = dR / dt$ is the velocity, and $k \approx \eta / a$ is a friction coefficient, with η the liquid viscosity and a the size of a monomer in the polymeric liquid. In this scenario, the rim has a circular cross-section. The resulting opening dynamics scale as $R \sim t^{2/3}$ (Redon et al. 1994).

It has been proposed that cellular dewetting resembles this latter scenario (Gonzalez-Rodriguez et al. 2012a, b). As the TEM opens, the rim advances over the substrate. Due to the disturbed cytoskeleton of intoxicated cells, adhesion with the substrate is reduced, and the membrane may slip over the substrate. This is the rationale to model friction dissipation in dewetting using Eq. (6.5). The friction coefficient k is expected to be of the order of $k \approx 10^8$ Pa.s.m.$^{-1}$, an estimate obtained from experiments that measured friction between a cell and a substrate (Guevorkian et al. 2010, Douezan and Brochard-Wyart 2011).

Different dynamics are observed in liquid dewetting on a slippery substrate and in cell dewetting, which is attributed to a different shape of the rim. The rim's cross-section is circular in the slippery liquid dewetting and flat in cellular dewetting. This difference modifies the equations of motion, leading to a cellular dewetting law that scales as $R \sim t^{1/2}$. Thus, cellular dewetting has diffusion-like opening dynamics, same as in the second liquid dewetting scenario discussed above. Interestingly, these two phenomena also share the common feature of a pancake-shaped rim. However, these apparent similarities correspond to different physics: the flat pancake rim in liquid dewetting is due to gravity effects, whereas in cell dewetting it is due to the cell's mechanical properties.

The cellular dewetting dynamics model summarized above is thus based on the assumptions of a pancake-shaped rim of constant height and membrane slipping on the substrate (Gonzalez-Rodriguez et al. 2012b). Its validity is supported by good agreement with the dynamics of opening observed in experiments. However, direct experimental investigation of the rim shape evolution is limited, and the flow field of the cell membrane during TEM opening has not been quantified. Future experiments could aim at experimentally characterizing these two aspects of TEM opening, in order to directly test the model's hypotheses.

6.3.7 Closure

Over longer time scales, of the order of several minutes, TEMs completely close down (Fig. 6.2).

Unlike transient pore closure in vesicles, the interplay between surface tension and line tension do not suffice to explain the dynamics of TEM closure, which is driven by extension of actomyosin-dependent processes. TEM closure has been related to the formation of lamellipodia-like projections via local Arp2/3-dependent branched-actin polymerization driven by MIM (Maddugoda et al. 2011). Closure driven by actin polymerization has been described by a physical model (Fedorov and Shemesh 2017). This model related actin polymerization dynamics to local curvature of the TEM edge. The model predicted that actin polymerization is slower in regions where the TEM edge has positive curvature (the curvature of a circular TEM) and faster in regions of negative curvature (such as a protrusion). This curvature effect is due to the effect of line tension, which promotes protrusion at a negatively curved edge, and to the lower compressive stress experienced by actin filaments in such regions, which results in a higher polymerization rate. The model successfully explains the observed instability of the circular TEM shape, which forms protrusions during the closure. The TEM closure mechanism described in this model does not require myosin motor activity for TEM repair.

An open question is the role of the actomyosin cable in the dynamics of TEM closure. Although a majority of the TEMs close by extension of membrane waves, we have also observed closure of TEMs by a purse-string phenomenon. Laser ablation experiments have shown that the cable after ablation retains its original length, indicating that it is under tension but does not undergo significant elastic deformation (Stefani et al. 2017). The absence of the contractility of the cable may dependent on the level of RhoA inactivation in intoxicated cells. In some circumstances the actomyosin cable that forms around the TEM (Stefani et al. 2017) could provide an additional mechanism to drive TEM closure by a purse-string mechanism similar to that described in wound healing of epithelial tissues (Vedula et al. 2015). In this case, it is not excluded that another type of contractile ring forms around TEMs when they stabilize prior to the closure by a purse-string mechanism.

6.4 Future Developments and Conclusions

In this section we discuss several physical phenomena observed in liquid dewetting for which an analogy in cellular dewetting has not yet been identified. These unexplored analogies, if pertinent, may lead to advancements in our understanding of the physics of TEMs.

6.4.1 Critical Thickness

Spontaneous dewetting of a liquid film on a solid substrate depends on the value of the spreading parameter S, which is the difference in energy between a wet patch and a dry patch (de Gennes et al. 2003). For $S > 0$ a liquid film is always stable and dewetting does not occur. For $S < 0$ dewetting occurs when the film thickness e is smaller than a critical threshold thickness e_c. The balance between capillarity and gravity defines this critical thickness. For $e < e_c$, a configuration where the liquid accumulates in patches of thickness e_c by leaving dry patches elsewhere is energetically favored, and dewetting can occur spontaneously. The continuous film of thickness $e < e_c$ is thus at a metastable state. Experiments perturbing the film destabilize its metastable state thereby initiating dewetting.

In cellular dewetting, the role of the liquid film is played by the whole cell. In the cell dewetting model, there is no direct analogy with the critical threshold thickness. This is because gravitational forces in liquid dewetting, which set the critical thickness, are negligible in cell dewetting, where they are much smaller than viscous and membrane forces. Nevertheless, it is observed that cellular dewetting occurs in cells that are abnormally thin, of the order of 50–100 nm or when pushing on the membranes to bring them in close proximity. This suggests the possible existence of a critical cell thickness for dewetting, although arising from different physics. Existence of a critical thickness would not simply mean that it is harder to nucleate a TEM in a thicker cell. Rather, we suggest that if the cell thickness is larger than a certain threshold, any nucleated

tunnel would immediately disappear, implying that TEM opening is observed only when the cell thickness is smaller than this threshold. In physics terms, the cell would be metastable below this critical thickness and stable above. In cellular dewetting, such critical thickness would not be set by gravity, but by a different force opposing TEM opening, such as actin cytoskeletal resistance.

6.4.2 Spinodal Dewetting

Very thin liquid films of $e < < e_c$ are unstable to capillary waves. Driven by van der Waals forces, perturbations get amplified at certain wavelengths, and the liquid films breaks up into multiple droplets. This dewetting mechanism is known as spinodal dewetting (Reiter 1992, de Gennes et al. 2003). It is a different dewetting mechanism from the nucleation and growth of dry patches.

Spinodal dewetting in cells has not been described. Whereas a direct physical analogy may not be pertinent, spinodal decomposition processes may play a role in cell dewetting. Similar to spinodal dewetting arising from the growth of surface perturbations in the liquid film, cellular dewetting appears to arise from perturbations in the cell membrane. Rather than studying out-of-plane perturbations of the film thickness like in spinodal liquid dewetting, it appears more pertinent to investigate heterogeneities in cell membrane composition. Indeed, spinodal decomposition leading to phase separation has been reported in multicomponent lipid vesicles (Veatch and Keller 2003). Such membrane heterogeneities may create preferential spots for TEM nucleation, as well as barriers between membrane domains that limit TEM opening. These considerations suggest studying how the locations of successive TEM opening within one cell correlate with heterogeneities in membrane composition.

In spinodal dewetting, a thin liquid film may be perturbed by the wavy topography of the substrate, if the wavelength of such geometrical substrate variations is large enough. Similarly, there could be a role of substrate geometry in cellular

dewetting. This analogy points to a possible effect of substrate patterning and of substrate curvature on inducing membrane perturbations and TEM nucleation. In the next section, we further consider how surface characteristics may affect cell dewetting.

6.4.3 Irregular and Soft Substrates

There are large variations in the fibrillar composition and mechanical properties of the extracellular matrix that is in direct contact with endothelial cells (Marchand et al. 2018). Substrate irregularities induce hysteresis in liquid dewetting (de Gennes et al. 2003). The origin for such hysteresis is the existence of two different contact angles for a drop placed on a textured surface, depending on whether the wetting front advances or recedes. Due to hysteresis, liquid dewetting on a textured surface may lead to stable configurations, where a dry patch keeps a constant size, and neither opens up nor closes. Hysteretic effects in cellular dewetting have not yet been described, but they could arise in cellular dewetting over patterned or heterogeneous substrates, which are known to significantly modify cell properties (Curtis and Wilkinson 1997, Anderson and Hinds 2011).

Liquid wetting and dewetting phenomena are also affected by substrate stiffness. If the substrate is sufficiently soft to be deformed by surface tension forces, elasto-capillary phenomena arise (Bico et al. 2018). To date, cellular dewetting on substrates of different stiffness has not been studied. However, we expect that substrate rigidity may affect cellular dewetting through physical mechanisms, such as elasto-capillarity, and through biological mechanisms, such as actin reorganization in response to mechanosensing. We also anticipate the role of biophysical mechanisms by which rigidity modifies the wetting properties of a substrate by a cell. It has been shown that the wetting of cellular aggregates can be equivalently modulated by substrate chemistry (as in classic liquid wetting) or by substrate rigidity (which is specific to biological wetting) (Douezan et al. 2012). Substrate coating and rigidity also affect wetting-

dewetting transitions in cellular monolayers (Perez-Gonzalez et al. 2019). Substrate coating and rigidity are known to affect the height of membrane undulations (Chang et al. 2017), which likely contribute to membrane collision for fusion and opening of TEMs. Taken together, these previous observations suggest an effect of substrate characteristics on cellular dewetting.

In conclusion, the analogy made between the dynamics of TEMs and the physics of liquid dewetting on non-wettable surfaces has been instrumental in deciphering essential parameters of TEM opening and stabilization. A challenge for the upcoming years will certainly encompass the comparison of this phenomenon to leukocyte diapedesis through the endothelium and the study of these phenomena in 3D models reflecting the physiological conditions of vessels. It will also be interesting to define the intrinsic cellular parameters that limit the formation of TEMs in cells. This should ultimately lead to progress in our understanding of spontaneous bleeding vascular diseases not due to platelet deficiencies.

References

Alon R, van Buul JD (2017) Leukocyte breaching of endothelial barriers: the actin link. Trends Immunol 38:606–615

Anderson DE, Hinds MT (2011) Endothelial cell micropatterning: methods, effects, and applications. Ann Biomed Eng 39(9):2329–2345

Bico J, Reyssat E, Roman B (2018) Elastocapillarity: when surface tension deforms elastic solids. Annu Rev Fluid Mech 50:629–659

Boyer L, Doye A, Rolando M, Flatau G, Munro P, Gounon P, Clément R, Pulcini C, Popoff MR, Mettouchi A, Landraud L, Dussurget O, Lemichez E (2006) Induction of transient macroapertures in endothelial cells through

RhoA inhibition by Staphylococcus aureus factors. J Cell Biol 173(5):809–819

Braakman ST, Pedrigi RM, Read AT, Smith JAE, Stamer WD, Ethier CR, Overby DR (2014) Biomechanical strain as a trigger for pore formation in Schlemm's canal endothelial cells. Exp Eye Res 127:224–235

Brochard-Wyart F, Redon C, Rondelez F (1988) Démouillage: régime de gravité. C R Acad Sci Paris 306(II):1143–1146

Cai Y, Rossier O, Gauthier NC, Biais N, Fardin MA, Zhang X, Miller LW, Ladoux B, Cornish VW, Sheetz MP (2010) Cytoskeletal coherence requires myosin-IIA contractility. J Cell Sci 123:413–423

Carman CV (2009) Mechanisms for transcellular diapedesis: probing and pathfinding by "invadosome-like protrusions.". J Cell Sci 122:3025–3035

Carman CV, Springer TA (2008) Trans-cellular migration: cell-cell contacts get intimate. Curr Opin Cell Biol 20:533–540

Carman CV, Sage PT, Sciuto TE, de la Fuente MA, Geha RS, Ochs HD, Dvorak HF, Dvorak AM, Springer TA (2007) Transcellular diapedesis is initiated by invasive podosomes. Immunity 26:784–797

Chang CH, Lee HH, Lee CH (2017) Substrate properties modulate cell membrane roughness by way of actin filaments. Sci Rep 7:9068

Chen CH, Tsai FC, Wang CC, Lee CH (2009) Three-dimensional characterization of active membrane waves on living cells. Phys Rev Lett 103(23):238101

Curtis A, Wilkinson C (1997) Topographical control of cells. Biomaterials 18(24):1573–1583

de Gennes PG, Brochard-Wyart D, Quéré D (2003) Capillarity and wetting phenomena. Drops, Bubbles, Pearls, Waves. Springer

Diz-Muñoz A, Fletcher DA, Weiner OD (2013) Use the force: membrane tension as an organizer of cell shape and motility. Trends Cell Biol 23(2):47–53

Douezan S, Brochard-Wyart F (2011) Spreading dynamics and wetting transition of cellular aggregates. Proc Natl Acad Sci USA 108(18):7315–7320

Douezan S, Brochard-Wyart F (2012) Dewetting of cellular monolayers. Eur Phys J E 35(5):34

Douezan S, Dumond J, Brochard-Wyart F (2012) Wetting transitions of cellular aggregates induced by substrate rigidity. Soft Matter 8(17):4578–4583

Fedorov EG, Shemesh T (2017) Physical model for stabilization and repair of trans-endothelial apertures. Biophys J 112(2):388–397

Fischer-Friedrich E, Hyman AA, Jülicher F, Muller DJ, Helenius J (2014) Quantification of surface tension and internal pressure generated by single mitotic cells. Sci Rep 4:6213

Forgacs G, Foty RA, Shafrir Y, Steinberg MS (1988) Viscoelastic properties of living embryonic tissues: a quantitative study. Biophys J 74(5):2227–2234

Gonzalez-Rodriguez D, Guevorkian K, Douezan S, Brochard-Wyart F (2012a) Soft matter models of developing tissues and tumors. Science 338:910–917

Gonzalez-Rodriguez D, Maddugoda MP, Stefani C, Janel S, Lafont F, Cuvelier D, Lemichez E, Brochard-Wyart F (2012b) Cellular dewetting: opening of macroapertures in endothelial cells. Phys Rev Lett 108(21):218105

Guevorkian K, Colbert MJ, Durth M, Dufour S, Brochard-Wyart F (2010) Aspiration of biological viscoelastic drops. Phys Rev Lett 104:218101

Helfrich W (1975) Out-of-plane fluctuations of lipid bilayers. Zeitschrift für Naturforschung C 30(11–12):841–842

Helfrich W, Servuss RM (1984) Undulations, steric interaction and cohesion of fluid membranes. Il Nuovo Cimento D 3(1):137–151

Karatekin E, Sandre O, Guitouni H, Borghi N, Puech PH, Brochard-Wyart F (2003) Cascades of transient pores in Giant vesicles: line tension and transport. Biophys J 84(3):1743–1749

Labernadie A, Bouissou A, Delobelle P, Balor S, Voituriez R, Proag A, Fourquaux I, Thibault C, Vieu C, Poincloux R, Charrière GM, Maridonneau-Parini I (2014) Protrusion force microscopy reveals oscillatory force generation and mechanosensing activity of human macrophage podosomes. Nat Commun 5:5343

Lemichez E, Gonzalez-Rodriguez D, Bassereau P, Brochard-Wyart F (2013) Transcellular tunnel dynamics: control of cellular dewetting by actomyosin contractility and I-BAR proteins. Biol Cell 105(3):109–117

Maddugoda MP, Stefani C, Gonzalez-Rodriguez D, Saarikangas J, Torrino S, Janel S, Munro P, Doye A, Prodon F, Aurrand-Lions M, Goossens PL, Lafont F, Bassereau P, Lappalainen P, Brochard F, Lemichez E (2011) cAMP signaling by anthrax edema toxin induces transendothelial cell tunnels, which are resealed by MIM via Arp2/3-driven actin polymerization. Cell Host Microbe 10(5):464–474

Maitre JL, Niwayama R, Turlier H, Nédélec F, Hiiragi T (2015) Pulsatile cell-autonomous contractility drives compaction in the mouse embryo. Nat Cell Biol 17(7):849–855

Marchand M, Monnot C, Muller L, Germain S (2018) Extracellular matrix scaffolding in angiogenesis and capillary homeostasis. Semin Cell Dev Biol S1084-9521(17):30578–30575

Mondal Roy S, Sarkar M (2011) Membrane fusion induced by small molecules and ions. J Lipids 2011: e528784

Munro P, Benchetrit M, Nahori MA, Stefani C, Clement R, Michiels JF, Landraud L, Dussurget O, Lemichez E (2010) Staphylococcus aureus EDIN toxin promotes formation of infection foci in a mouse model of bacteremia. Infect Immun 78:3404–3411

Ng WP, Webster KD, Stefani C, Schmid EM, Lemichez E, Bassereau P, Fletcher DA (2017) Force-induced transcellular tunnel formation in endothelial cells. Mol Biol Cell 28(20):2589–2745

Oakes PW, Banerjee S, Marchetti MC, Gardel ML (2014) Geometry regulates traction stresses in adherent cells. Biophys J 107(4):825–833

Oldewurtel ER, Kouzel N, Dewenter L, Henseler K, Maier B (2015) Differential interaction forces govern bacterial sorting in early biofilms. elife 4:e10811

Pérez-González C, Alert R, Blanch-Mercader C, Gómez-González M, Kolodziej T, Bazellieres E, Casademunt J, Trepat X (2019) Active wetting of epithelial tissues. Nat Phys 15:79–88

Phillips HM, Steinberg MS (1978) Embryonic tissues as elasticoviscous liquids. I. Rapid and slow shape changes in centrifuged cell aggregates. J Cell Sci 30:1–20

Raucher D, Sheetz MP (2000) Cell spreading and lamellipodial extension rate is regulated by membrane tension. J Cell Biol 148:127–136

Redon C, Brochard-Wyart F, Rondelez F (1991) Dynamics of dewetting. Phys Rev Lett 66(6):715–718

Redon C, Brzoska JB, Brochard-Wyart F (1994) Dewetting and slippage of microscopic polymer films. Macromolecules 27:468–471

Reiter G (1992) Dewetting of thin polymer films. Phys Rev Lett 68(1):75–78

Rühs PA, Böni L, Fuller GG, Inglis RF, Fischer P (2013) In-situ quantification of the interfacial rheological response of bacterial biofilms to environmental stimuli. PLoS One 8(11):e78524

Saarikangas J, Zhao H, Pykalainen A, Laurinmaki P, Mattila PK, Kinnunen PK, Butcher SJ, Lappalainen P (2009) Molecular mechanisms of membrane deformation by I-BAR domain proteins. Curr Biol 19:95–107

Sackmann E, Bruinsma RF (2002) Cell adhesion as wetting transition? Chem Phys Chem 3:262–269

Sandre O, Moreaux L, Brochard-Wyart F (1999) Dynamics of transient pores in stretched vesicles. Proc Natl Acad Sci USA 96(19):10591–10596

Sheetz MP, Dai J (1996) Modulation of membrane dynamics and cell motility by membrane tension. Trends Cell Biol 6:85–89

Shi Z, Graber ZT, Baumgart T, Stone HA, Cohen AE (2018) Cell membranes resist flow. Cell 175:1769–1779

Stefani C, Gonzalez-Rodriguez D, Senju Y, Doye A, Efimova N, Janel S, Lipuma J, Tsai MC, Hamaoui D, Maddugoda MP, Cochet-Escartin O, Prévost C, Lafont F, Svitkina T, Lappalainen P, Bassereau P, Lemichez E (2017) Ezrin enhances line tension along transcellular tunnel edges via NMIIa driven actomyosin cable formation. Nat Commun 23(8):15839

Steinberg MS (1963) Reconstruction of tissues by dissociated cells. Science 141(3579):401–408

Tsai FC, Bertin A, Bousquet H, Manzi J, Senju Y, Tsai MC, Picas L, Miserey-Lenkei S, Lappalainen P, Lemichez E, Coudrier E, Bassereau P (2018) Ezrin enrichment on curved membranes requires a specific conformation or interaction with a curvature-sensitive partner. Elife 7:e37262

Veatch SL, Keller SL (2003) Separation of liquid phases in Giant vesicles of ternary mixtures of phospholipids and cholesterol. Biophys J 85(5):3074–3083

Vedula SR, Peyret G, Cheddadi I, Chen T, Brugués A, Hirata H, Lopez-Menendez H, Toyama Y, de Almeida LN, Trepat X, Lim CT, Ladoux B (2015) Mechanics of epithelial closure over non-adherent environments. Nat Commun 6:6111

Yeung A, Evans E (1989) Cortical shell-liquid core model for passive flow of liquid-like spherical cells into micropipets. Biophys J 56:139–149